

10. A gasketed Mao-Bell type DAC was used with anvils having 200- μm culets [H. K. Mao, P. M. Bell, K. J. Dunn, R. M. Chrenko, R. C. DeVries, *Rev. Sci. Instrum.* **50**, 1002 (1979)]. The gasket was spring steel, and the sample diameter under pressure was ~ 80 μm . The sample was heated by means of a continuous (cw) Nd:YAG (Nd:yttrium-aluminum-garnet) laser operating in multi-mode (wavelength of 1064 nm), as described by A. Kavner and R. Jeanloz [in *Advanced Materials '96*, M. Akaishi *et al.*, Eds. (NIRIM, Tsukuba, Japan, 1996), pp. 143–147]. The laser beam was focused to a diameter of ~ 15 μm and scanned to heat the entire sample. X-ray diffraction patterns were collected in angular-dispersive mode at beamline 10-2 of the Stanford Synchrotron Radiation Laboratory (SSRL), using a monochromatized x-ray beam of 17.038 keV with an imaging-plate detector. Because the diameter of the incident x-ray beam was slightly larger than that of the sample, diffraction line or lines from the gasket were present in the patterns we collected. The imaging-plate data were converted to a 2 θ -intensity profile, using the program developed by J. H. Nguyen and R. Jeanloz [*Rev. Sci. Instrum.* **64**, 3456 (1993)]. All x-ray diffraction measurements were carried out at room temperature.
11. See, for example, W. A. Caldwell *et al.*, *Science* **277**, 930 (1997).
12. Because the equation of state of Pt is well known, pressure can be calculated from the unit-cell volume of Pt measured by x-ray diffraction [N. C. Holmes, J. A. Moriarty, G. R. Gathers, W. J. Nellis, *J. Appl. Phys.* **66**, 2962 (1989)].
13. See, for example, D. Heinz and R. Jeanloz, *J. Geophys. Res.* **92**, 11437 (1987).
14. Pressure or temperature gradients, or both, in the sample chamber (9, 13) may have resulted in the existence of untransformed $\alpha\text{-Al}_2\text{O}_3$.
15. $\text{Al}^{(1)} = (0.110, 0.753, 0.032)$, $\text{O}^{(1)} = (0.846, 0.607, 0.102)$, $\text{O}^{(2)} = (0.000, 0.049, 0.250)$ (7).
16. R. J. Hemley *et al.*, *Science* **276**, 1242 (1997). Because we did not heat the gasket, it may have retained a large uniaxial stress.
17. Transformations from $\alpha\text{-Al}_2\text{O}_3$ to phases of unknown structure at 16 to 21 GPa and 1600 to 1900 K have been proposed, based on optical observations on quenched samples [T. Gasparik, *J. Geophys. Res.* **95**, 15751 (1990)]. Experimental details have not been reported, but the high-pressure phase documented here is likely to be different, because it cannot be quenched to ambient pressure. In a separate experiment, we have tentative evidence for the appearance of the Rh_2O_3 (II) phase when ruby is heated at a pressure as low as ~ 85 GPa.
18. To avoid such problems in ultra-high pressure experiments with the laser-heated DAC, attempts are usually made to obtain ruby-fluorescence determinations of pressure from portions of the sample that have been heated as little as possible. See E. Knittle and R. Jeanloz, *Science* **235**, 668 (1987); Q. Williams, E. Knittle, R. Jeanloz, *J. Geophys. Res.* **96**, 2171 (1991); (3); and (7).
19. P. A. Urtiew, *J. Appl. Phys.* **45**, 3490 (1974); C. S. Yoo, N. C. Holmes, M. Ross, D. J. Webb, C. Pike, *Phys. Rev. Lett.* **70**, 3931 (1993).
20. D. Erskine's [in *High-Pressure Science and Technology—1993*, part I, S. C. Schmidt *et al.*, Eds. (American Institute of Physics, Woodbury, NY, 1994), pp. 141–143] shock-wave equation of state (Hugoniot) measurements on single-crystal Al_2O_3 are described by $U_S = 8.74 + 0.96 u_p$ between 80 and 340 GPa, where U_S and u_p are shock-wave velocity and particle velocity, respectively, and all values are in km/s. On the basis of its elastic properties (9, 21), $\alpha\text{-Al}_2\text{O}_3$ is expected to follow $U_S = 7.93 + 1.32 u_p$ [see R. Jeanloz, *J. Geophys. Res.* **94**, 5873 (1989)], and the data of (21) are found to be compatible with this for u_p between about 1.6 and 2.5 km/s (strength effects probably explain higher shock-wave velocities for $u_p < 1.6$ km/s). The intersection of these two U_S - u_p relations, $u_p = 2.25$ km/s, can be combined with the Hugoniot momentum-conservation relation to obtain a pressure of 98 GPa at which the shock-wave data begin to deviate toward a new (high-pressure phase) branch of the Hugoniot. This is in good agreement with the pressure at which we find evidence for the crystal-structural transformation of Al_2O_3 . Also, a theoretical Hugoniot calculated for the Rh_2O_3 (II) phase matches the U_S - u_p relation measured by Erskine for Al_2O_3 at pressures above 100 GPa.
21. S. P. Marsh, Ed., *LASL Shock Hugoniot Data* (Univ. of California Press, Berkeley, CA, 1980).
22. A. P. Jephcoat, H. K. Mao, P. M. Bell, *J. Geophys. Res.* **91**, 4677 (1986).
23. We are grateful to M. S. T. Bukowski, T. Uchida, J. H. Nguyen, W. A. Caldwell, L. R. Benedetti, and staff members at SSRL for helpful discussions and experimental support. Supported by NSF, NASA, and the Miller Institute for Basic Research in Science (Berkeley, CA).

5 August 1997; accepted 7 October 1997

Direct Measurement of Distances and Angles in Biomolecules by NMR in a Dilute Liquid Crystalline Medium

Nico Tjandra and Ad Bax

In isotropic solution, internuclear dipolar couplings average to zero as a result of rotational diffusion. By dissolving macromolecules in a dilute aqueous nematic discotic liquid-crystalline medium containing widely spaced magnetically oriented particles, a tunable degree of solute alignment with the magnetic field can be created while retaining the high resolution and sensitivity of the regular isotropic nuclear magnetic resonance (NMR) spectrum. Dipolar couplings between ^1H - ^1H , ^1H - ^{13}C , ^1H - ^{15}N , and ^{13}C - ^{13}C pairs in such an oriented macromolecule no longer average to zero, and are readily measured. Distances and angles derived from dipolar couplings in human ubiquitin are in excellent agreement with its crystal structure. The approach promises to improve the accuracy of structures determined by NMR, and extend the size limit.

Internuclear magnetic dipole couplings contain a great deal of structural information, but in isotropic solution, they average to zero as a result of rotational diffusion. However, their effect on nuclear spin relaxation results in measurable nuclear Overhauser effects (NOEs). These NOEs are commonly interpreted in terms of qualitative internuclear distances, which constitute the basis for macromolecular structure determination by NMR (1). The qualitative manner in which interprotein distances are derived from NOEs limits the accuracy at which the time-averaged conformation of biomolecules can be determined. Moreover, the cumulative error in these local constraints can make it difficult to determine the relative positions of structural elements with few connecting NOEs.

These problems can be addressed by making use of the minute degree of molecular alignment that occurs for proteins with a nonzero magnetic susceptibility anisotropy when they are placed in a strong magnetic field (2–5). Such alignment can result in measurable values of the one-bond ^{15}N - ^1H and ^{13}C - ^1H dipolar couplings. Because the internuclear distance for these dipolar

interactions is essentially fixed, the dipolar couplings provide direct information on the orientations of the corresponding bond vectors relative to the protein's magnetic susceptibility tensor. These constraints are therefore fundamentally different from the strictly local NOE and J coupling constraints. Addition of only 90 such dipolar constraints, measured for a small protein complexed with a 16–base pair DNA fragment, resulted in a nearly twofold reduction of ϕ - ψ pairs (torsion angles) outside of the most-favored region of the Ramachandran map (5) and greatly improved the agreement between predicted and measured magnetic field dependence of ^{15}N shifts (6). Unfortunately, the magnetic interaction energy for an individual macromolecule is generally so weak that only in favorable systems, and with considerable effort, can these dipolar couplings be measured with sufficient accuracy. Here we demonstrate a simple and general method for inducing alignment of biomolecules with the magnetic field: the use of an aqueous, dilute, liquid crystalline (LC) phase. This method yields an adjustable degree of molecular alignment and allows not only ^1H - ^{15}N , but also many other types of dipolar interactions to be measured directly and with high accuracy.

Although LC media have long been used for orienting solutes in order to study their structure (7–9), the degree of solute orientation typically obtained in such a sol-

N. Tjandra, Laboratory of Biophysical Chemistry, National Heart, Lung, and Blood Institute, National Institutes of Health, Bethesda, MD 20892–0380, USA.

A. Bax, Laboratory of Chemical Physics, National Institute of Diabetes and Digestive and Kidney Diseases, National Institutes of Health, Bethesda, MD 20892–0520, USA.

vent is so large that the NMR spectra of molecules with more than a dozen hydrogens become too complex to interpret. Recently, numerous compounds that form ordered LC arrays at low volume fractions in water have been identified (10–12). We focus here on discotic phospholipid micelles, which consist of mixtures (1:2.9 in our case) of dihexanoyl phosphatidylcholine (DHPC) and dimyristoyl phosphatidylcholine (DMPC) (11). In aqueous solution at or just above room temperature, these lipids switch from a gel to an LC phase, where they form disc-shaped particles, often referred to as bicelles, with diameters of several hundred angstroms and thicknesses of ~ 40 Å (11, 13). The lipids are diamagnetic, and, as a result, the bicelles orient with their normal orthogonal to the magnetic field.

Important structural information has

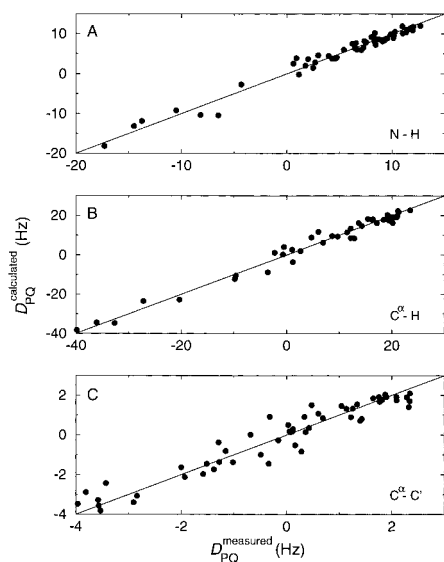


Fig. 1. Correlation between the measured one-bond dipolar splittings in human ubiquitin and values predicted on the basis of its 1.8 Å x-ray crystal structure, using $SA_a = 8.3 \times 10^{-4}$ and $SA_r = 1.4 \times 10^{-4}$; the orientation of the alignment tensor in the frame of the PDB x-ray structure coordinates (1UBQ) is defined by the Euler angles $\alpha = 41^\circ$, $\beta = 35^\circ$, and $\gamma = -41^\circ$. (A) $^1\text{H}-^{15}\text{N}$, (B) $^1\text{H}-^{13}\text{C}^\alpha$, and (C) $^{13}\text{C}^\alpha-^{13}\text{C}^\gamma$ dipolar couplings. The plot assumes that the same order parameter applies to all three types of couplings. Dipolar couplings in residues for which previously (22) a low order parameter ($S^2 < 0.7$) was measured for the backbone amide have absolute values smaller than predicted by the crystal structure and are not included in the figure. Uncertainties in the measured dipolar couplings are (A) 0.5 Hz, (B) 1 Hz, and (C) 0.5 Hz. The sample contained 0.3 mM ubiquitin, 5% w/v lipid (in a 2.9:1 molar ratio of DMPC:DHPC), pH 6.8. Dipolar couplings were obtained from the difference between splittings measured in the oriented phase (at 38°C) and in the isotropic phase (25°C), both carried out at 750-MHz ^1H frequency.

been obtained from NMR studies of small molecules anchored in such oriented bicelles, typically at bicelle concentrations that are as high as possible (14). However, the LC phase can also be maintained at low volume fractions, of at least 3% w/v, and the high degree of magnetic alignment of these particles persists at these low concentrations (12, 15). In such a dilute LC phase, the spacing between individual bicelles is far greater than the size of the macromolecules typically studied by NMR. As a result, and in contrast to the small molecules anchored in such bilayers, they can diffuse freely in the aqueous solvent. The ^{15}N transverse relaxation rates in the protein ubiquitin (76 residues, 8.6 kD) are barely affected by the presence of the bicelles, indicating that rotational diffusion occurs at the same rate (15). However, ubiquitin's deviation from a spherical shape results in a small, tunable degree of protein alignment in such an anisotropic medium.

In full analogy to the case of magnetic susceptibility anisotropy, where dipolar couplings define the orientation of the interaction relative to the magnetic susceptibility tensor, we define a molecular alignment tensor \mathbf{A} , which can be decomposed into an axially symmetric component A_a and a rhombic component A_r (16). The magnitude and orientation of \mathbf{A} is not known a priori but is determined from the measured dipolar couplings. The observed residual dipolar coupling between two nuclei, P and Q, is given by

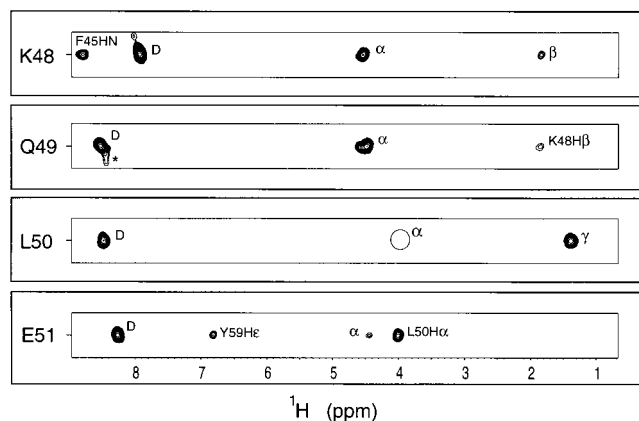
$$D_{PQ}(\theta, \phi) = S \frac{\mu_0}{4\pi} \gamma_P \gamma_Q h \left[A_a (3 \cos^2 \theta - 1) + \frac{3}{2} A_r \sin^2 \theta \cos 2\theta \right] / 4\pi^2 r_{PQ}^3 \quad (1)$$

where \mathbf{S} is the generalized order parameter for internal motion of the vector PQ (5, 17, 18), μ_0 is the magnetic permeability of vacuum, γ_P and γ_Q are the magnetogyric ratios of P and Q, h is Planck's constant, r_{PQ} is the distance between P and Q, and θ and ϕ are cylindrical coordinates describing the orientation of the PQ vector in the principal axis system of \mathbf{A} . Values of S^2 obtained from ^{15}N or ^{13}C relaxation experiments typically range from 0.7 to 0.9, that is, \mathbf{S} falls between 0.85 and 0.95. Values for A_a and A_r depend on the shape of the protein and vary with the bicelle concentration (15), which is adjusted to yield an A_a of $\sim 10^{-3}$.

For such small alignment values, only dipolar couplings between nearby nuclei give rise to observable splittings, which keeps the NMR spectrum simple. If there is also a scalar coupling J between the two nuclei, the observed splitting corresponds to $J_{PQ} + D_{PQ}$. For one-bond $^1\text{H}-^{13}\text{C}$, $^1\text{H}-^{15}\text{N}$, or $^{13}\text{C}-^{13}\text{C}$ interactions, J_{PQ} is relatively large and its sign is known. The change in the observed splitting upon changing from the isotropic to the aligned phase then yields the magnitude and sign of D_{PQ} (19). For pairs of protons that are not J coupled, only the magnitude of D_{PQ} is obtained, and additional experiments (20) need to be developed to obtain information about the sign of this coupling.

Figure 1 shows the excellent agreement between dipolar couplings measured in human ubiquitin and those predicted by its 1.8 Å x-ray crystal structure (21). Assuming a uniform order parameter, \mathbf{S} , for internal motion, the orientation and magnitude of the alignment tensor (five adjustable parameters) was determined in the same manner as previously described for its rotational diffusion tensor (22), yielding $SA_a = 8.3 \times 10^{-4}$ and $SA_r = 1.4 \times 10^{-4}$. This value is two

Fig. 2. Strip cross sections taken parallel to the F_2 axis through the 600-MHz three-dimensional HNHA spectrum (26) of human ubiquitin (VLI Research, Southeastern, PA), at the (F_1, F_3) positions of the amides of residues Lys⁴⁸-Glu⁵¹, recorded with a $^1\text{H}-^1\text{H}$ dephasing time of 21.6 ms. The cross sections display resonances of protons coupled to these amide protons, and the intensity ratio of the cross peak and the corresponding diagonal resonance, marked D, permits straightforward calculation of the magnitude of the interaction. For the intrasidue $\text{H}^{\text{N}}-\text{H}^\alpha$ interactions, the cross-peak intensity corresponds to the sum of $J_{\text{HNH}\alpha}$ and $D_{\text{HNH}\alpha}$. Cross-peak labels α , β , and γ refer to intrasidue cross peaks to H^α , H^β , and H^γ protons. The open circle for Leu⁵⁰ marks the position of the intrasidue $\text{H}^{\text{N}}-\text{H}^\alpha$ cross peak, not observed as a result of the near-zero value of $J_{\text{HNH}\alpha} + D_{\text{HNH}\alpha}$.



orders of magnitude greater than its magnetic alignment at the highest available magnetic field strengths (3). The orientation of the axial component of the alignment tensor agrees closely with that of the nearly axially symmetric rotational diffusion tensor (22), confirming that the alignment is caused by the interaction between the protein's hydrodynamic properties and the deviation from spherical symmetry of the medium in which it is dissolved. Small differences between the measured values of D_{NH} and D_{CH} and the values predicted by the crystal structure (Fig. 1) reflect slightly different orientations of the corresponding internuclear vectors in the protein in free solution and in the crystal structure, to which hydrogens were added with the program X-PLOR (23). The program positions the amide hydrogens in the $C'_{i-1}-N_i-C^\alpha_i$ plane, but small deviations from such a planar arrangement are known to occur (24). In this respect, it is interesting to note that for θ in the 30° to 60° range, a change in θ of only 1° results in a ~ 0.5 -Hz change in D_{NH} (compare with Eq. 1), which is approximately equal to the experimental uncertainty in the measurement.

For a protein of unknown structure, a reasonable estimate for A_a can be obtained from the range of dipolar couplings observed. The value of A_r can be determined in a stepwise iterative manner. In contrast, the orientation of the alignment tensor floats freely during structure calculations (5, 25).

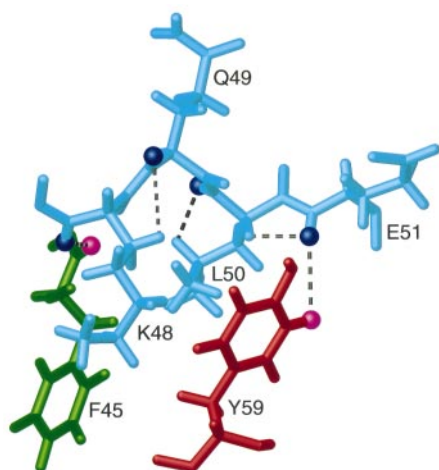


Fig. 3. Small region of the ubiquitin crystal structure, displaying the atoms of residues Lys⁴⁸ through Glu⁵¹ (light blue; backbone amide protons, dark blue), Phe⁴⁵ (green), and Tyr⁵⁹ (red). Protons on these last two residues with long-range interactions to Lys⁴⁸-H^N and Glu⁵¹-H^N are shown in magenta. Interresidue dipolar interactions are marked by dashed lines. The molecular fragment is shown in the coordinate frame of the alignment tensor. The figure was made with the program MOLMOL (29).

For directly bonded pairs of atoms, the internuclear distance is accurately known, and the measured dipolar coupling provides information on the orientation of the internuclear bond vector. Dipolar interactions can also be measured between pairs of protons that are separated by many chemical bonds. For example, Fig. 2 shows several small strips taken from the three-dimensional HNHA spectrum (26), normally used to measure $J_{\text{HNH}\alpha}$ couplings in proteins. Besides the intraresidue coupling between H ^{α} and the detected H^N resonance, numerous long-range interactions mediated by dipolar couplings are also observed in this spectrum. For example, the amide proton of Glu⁵¹ shows dipolar couplings to Tyr⁵⁹-H ^{ϵ} and to H ^{α} of Leu⁵⁰. For Leu⁵⁰, no interaction to its H ^{α} is observed, indicating that $J_{\text{HNH}\alpha}$ and $D_{\text{HNH}\alpha}$ have opposite signs and nearly cancel one another; an intense interaction to H ^{γ} indicates a large value for $D_{\text{HNH}\gamma}$. These interactions correspond to hydrogens proximate to Glu⁵¹-H^N with the interproton vector outside of the $\theta = 54^\circ \pm 10^\circ$ range (Fig. 3). No correlation is observed to Glu⁵¹-H ^{β} ($r_{\text{HH}} = 2.9$ Å; $\theta = 46^\circ$) because the interproton vector is oriented close to the “magic” angle ($\theta = 54.7^\circ$), where the A_a contribution to D_{HH} (Eq. 1) equals zero.

The degree of protein alignment in the LC medium is a function of its shape. Ubiquitin's deviation from isotropic rotational diffusion is quite small (22), and most biological macromolecules will show somewhat greater degrees of alignment (27). Measurement of dipolar couplings requires less sample than detection of weak NOEs, and only small amounts of labeled proteins (0.1 to 0.5 mM) were used in these measurements. However, experiments using unlabeled material indicate that, for most proteins, the LC phase is not affected by concentrations as high as 5 mM. We have already demonstrated the large improvement in structural quality obtained upon adding such dipolar constraints to the NMR structure calculation (5). They were shown to contain unique “long-range” information not available from NOEs or J couplings, as they orient all vectors relative to a single axis system.

For none of the systems studied so far have we found any significant changes in chemical shift upon addition of the lipids. This result indicates that there are no stable, direct interactions between the lipids and the macromolecules, and no reassignment of the NMR spectrum is needed. Small changes in chemical shift between the LC and isotropic states [$\leq \sim 0.1$ parts per million (ppm) for ¹⁵N and ¹³C; $\leq \sim 0.01$ ppm for ¹H] result from incomplete averaging of chemical shift anisotropy (CSA) in the aligned state. In principle, it is possible to separate this CSA effect from the tem-

perature dependence of the chemical shift, thereby providing access to the potentially important structural information contained in the CSA tensor (6).

The degree of protein alignment obtained at low bicelle concentrations is large enough to accurately measure a wide array of dipolar couplings, yet small enough to prevent crowding and attenuation of the spectrum by the multitudes of dipolar couplings typically encountered in regular LC NMR (7–9). The dipolar couplings yield structural information of an accuracy that is unprecedented in macromolecular NMR and will undoubtedly increase the quality of structures dramatically. The approach also holds the potential of extending NMR structure determination to proteins beyond 30 kD. For such proteins, resonance assignments can frequently be made, but the small number of measurable long-range NOEs, typically involving methyl groups and amide protons (28), are insufficiently constraining to calculate a satisfactory structure. Addition of ¹H-¹⁵N and ¹³C-¹³C dipolar couplings, which are readily measured in perdeuterated proteins, is likely to add sufficient constraining information for determining such a structure at a reasonable level of resolution. Measurement and identification of dipolar couplings in a dilute LC medium is a fast and straightforward process. It is not restricted to biological macromolecules and should be immediately applicable to numerous other types of molecules, including carbohydrates, peptides, and natural products.

REFERENCES AND NOTES

1. K. Wüthrich, *NMR of Proteins and Nucleic Acids* (Wiley, New York, 1986); G. M. Clore and A. M. Gronenborn, *Crit. Rev. Biochem. Mol. Biol.* **24**, 479 (1989).
2. J. R. Tolman, J. M. Flanagan, M. A. Kennedy, J. H. Prestegard, *Proc. Natl. Acad. Sci. U.S.A.* **92**, 9279 (1995); H. C. Kung, K. Y. Wang, I. Goljer, P. H. Bolton, *J. Magn. Reson. B* **109**, 323 (1995).
3. N. Tjandra, S. Grzesiek, A. Bax, *J. Am. Chem. Soc.* **118**, 6264 (1996).
4. J. R. Tolman and J. H. Prestegard, *J. Magn. Reson. B* **112**, 245 (1996); N. Tjandra and A. Bax, *J. Magn. Reson.* **124**, 512 (1997).
5. N. Tjandra, J. G. Omichinski, A. M. Gronenborn, G. M. Clore, A. Bax, *Nature Struct. Biol.* **4**, 732 (1997).
6. M. Ottiger, N. Tjandra, A. Bax, *J. Am. Chem. Soc.* **119**, 9825 (1997).
7. A. Saupe and G. Englert, *Phys. Rev. Lett.* **11**, 462 (1963).
8. J. W. Emsley and J. C. Lindon, *NMR Spectroscopy Using Liquid Crystal Solvents* (Pergamon, New York, 1975).
9. P. Diehl, in *Nuclear Magnetic Resonance of Liquid Crystals*, J. W. Emsley, Ed. (Reidel, Dordrecht, Netherlands, 1985), pp. 147–180.
10. N. Boden, S. A. Corne, K. W. Jolley, *J. Phys. Chem.* **91**, 4092 (1987); P. Ram and J. H. Prestegard, *Biochim. Biophys. Acta* **940**, 289 (1988).
11. C. R. Sanders and J. P. Schwonek, *Biochemistry* **31**, 8898 (1992).
12. W. J. Harrison, D. L. Mateer, G. J. T. Tiddy, *Faraday Discuss.* **104**, 139 (1996).

13. R. R. Vold and P. S. Prosser, *J. Magn. Reson. B* **113**, 267 (1996).
14. C. R. Sanders, B. J. Hare, K. P. Howard, J. H. Prestegard, *Prog. Nucl. Magn. Reson. Spectrosc.* **26**, 421 (1994); G. Metz *et al.*, *J. Am. Chem. Soc.* **117**, 564 (1995).
15. A. Bax and N. Tjandra, *J. Biomol. NMR* **10**, 289 (1997).
16. In the LC literature, this alignment tensor is usually referred to as **S** (β), but to avoid confusion with the order parameter for internal motion, commonly also denoted **S** (17), we refer to it as **A**.
17. G. Lipari and A. Szabo, *J. Am. Chem. Soc.* **104**, 4546 (1982).
18. J. R. Tolman, J. M. Flanagan, M. A. Kennedy, J. H. Prestegard, *Nature Struct. Biol.* **4**, 292 (1997).
19. One-bond *J* splittings are measured in the unoriented phase at 25°C—just below the temperature of the phase transition from gel to liquid crystal—and in the LC phase at 38°C.
20. C. Griesinger, O. W. Sørensen, R. R. Ernst, *J. Chem. Phys.* **85**, 6837 (1986).
21. S. Vijay-Kumar, C. E. Bugg, W. J. Cook, *J. Mol. Biol.* **194**, 531 (1987).
22. N. Tjandra, S. E. Feller, R. W. Pastor, A. Bax, *J. Am. Chem. Soc.* **117**, 12562 (1995).
23. A. T. Brünger, *X-PLOR Version 3.1: A System for X-ray Crystallography and NMR* (Yale Univ. Press, New Haven, CT, 1992).
24. M. W. MacArthur and J. M. Thornton, *J. Mol. Biol.* **264**, 1180 (1996).
25. N. Tjandra, D. S. Garrett, A. M. Gronenborn, A. Bax, G. M. Clore, *Nature Struct. Biol.* **4**, 443 (1997).
26. G. W. Vuister and A. Bax, *J. Am. Chem. Soc.* **115**, 7772 (1993).
27. Spectra showing the dipolar coupling contributions in other systems—a DNA dodecamer, the GATA1-DNA complex, and calmodulin—can be found at <http://www.sciencemag.org/feature/data/974460.shl>
28. L. E. Kay and K. H. Gardner, *Curr. Opin. Struct. Biol.* **7**, 722 (1997).
29. R. Koradi, M. Billeter, K. Wüthrich, *J. Mol. Graphics* **14**, 52 (1996).
30. We thank M. Clore, W. Eaton, J. Emsley, J. Ferretti, K. Gawrisch, A. Gronenborn, W. Hagsin, J. Hofrichter, I. Levin, A. Parsegian, D. Rao, O. Soderman, and A. Szabo for many stimulating discussions and useful suggestions; F. Delaglio and D. Garrett for software support; J. Omichinski for providing us the ¹⁵N-GATA1-DNA complex; and M. Kainosho, S. Tate, and A. Ono (Tokyo Metropolitan University) for the d(CGCGAA{¹³C}-TTCCGG)₂ DNA dodecamer shown in (27). Supported by the Intramural AIDS Targeted Anti-Viral Program of the Office of the Director of the National Institutes of Health.

15 August 1997; accepted 1 October 1997

Lake Baikal Record of Continental Climate Response to Orbital Insolation During the Past 5 Million Years

D. F. Williams,* J. Peck, E. B. Karabanov, A. A. Prokopenko, V. Kravchinsky, J. King, M. I. Kuzmin

The sedimentary record of biogenic silica from Lake Baikal in south-central Siberia suggests that this region of central Asia was impacted by two major cooling episodes at 2.8 to 2.6 and 1.8 to 1.6 million years ago. The spectral evolution of this continental interior site parallels the evolutionary frequency spectra for various marine oxygen isotope records. In the Baikal record, the 41,000-year obliquity cycle is particularly strong from 1.8 to 0.8 million years ago; variance in the 100,000-year eccentricity band increases during the past 0.8 million years. The expected precession frequency of 23,000 years is highest during the past 400,000 years. The modulation of the predicted 23,000- and 41,000-year insolation forcing by the 100,000- and 400,000-year eccentricity bands indicates that the transfer of variance from the precession and obliquity frequencies to the eccentricity part of the spectrum occurred in the Eurasian continental interior, as well as in tropical and high-latitude ocean sites.

Simulations of the response of Earth's climate system to changes in both external (1–3) and internal boundary conditions (4–9) have led to new understanding of the evolution of the Asian monsoonal system and African and Arabian continental aridity and moisture patterns through time. The general pattern of the Asian climate response for the past 30 thousand years (ky) is

fairly well known from lake piston cores (10), and for the past 2.6 million years (Ma), it is known from the Chinese loess sections (11, 12). However, long, high-resolution sedimentary sections with multiple climate proxies have not been available for the high-latitude, continental interior regions of central Eurasia. Energy balance modeling (3) has suggested that the temperature responses of this region may have been as high as 14°C during glacial-interglacial fluctuations of the past 800 ky. These model projections are based on a linear response to orbitally induced variations in seasonal insolation due to the 23-ky precession cycle with some contribution from the 41-ky obliquity cycle according to the Milankovitch theory (13). The recent recovery of sedimentary records for the past 5 Ma from Lake Baikal, in south-central Siberia (14), provided an opportunity to test climate model projections on the response of central Eurasian watersheds and ecosystems to external orbital forcing and

internal climate system feedbacks, as well as to provide a stratotype for continental paleoclimate studies.

Lake Baikal is the world's largest and deepest freshwater lake (15). Because Lake Baikal is located in the continental interior, its hydrodynamic system and biological productivity are sensitive to solar energy variations (16), which in turn are accurately recorded through the flux of biogenic silica and diatom abundance to the bottom sediments (17–20). To develop an understanding of Baikal's response to paleoclimate processes, we adopted a strategy similar to that used in the study of marine records by studying Baikal cores with multiple climate proxies (21–23) and detailed accelerator mass spectrometry radiocarbon dates for the past 25 ky (24, 25). Spectral analysis of records spanning the past 250 ky (22, 25) has provided evidence that orbital frequencies are embedded in and resolvable from the Baikal record (26).

From January to April 1996, a Russian scientific drilling team successfully recovered a sedimentary record spanning the past 5 Ma from a deep-water topographic high known as the Academician Ridge (27). In Baikal Drilling Program 1996 (BDP-96) hole 1, 93% of the core was recovered in the upper 119 m. Because rotary drilling was used to complete drilling to a total subbottom depth of 300 m, coring recovery averaged 61% from 119 to 192 m subbottom (for technical reasons, only logging was done between 192 and 300 m). In hole 2, 99% of the core was recovered with an advanced hydraulic piston corer (APC) to a subbottom depth of 100 m. Comparison of detailed inclination profiles for holes 1 and 2 with a reference geomagnetic polarity time scale for the Neogene (Fig. 1, A through C) (28–30) reveals that the basal age is about 5 Ma; robust reversal boundaries provide 13 age control points. A plot of the age-depth relation based on these geomagnetic polarity boundaries shows that the hemipelagic accumulation rate is a nearly constant 4 cm

D. F. Williams, Department of Geological Sciences, University of South Carolina, Columbia, SC 29208, USA.

J. Peck and J. King, Graduate School of Oceanography, University of Rhode Island, Narragansett, RI 02882, USA.

E. B. Karabanov, Department of Geological Sciences, University of South Carolina, Columbia, SC 29208, USA, and Institute of Geochemistry, Russian Academy of Science (Siberian Branch), Irkutsk, Russia.

A. A. Prokopenko, Department of Geological Sciences, University of South Carolina, Columbia, SC 29208, USA, and United Institute of Geology, Geochemistry and Mineralogy, Russian Academy of Science (Siberian Branch), Novosibirsk, Russia.

V. Kravchinsky and M. I. Kuzmin, Institute of Geochemistry, Russian Academy of Science (Siberian Branch), Irkutsk, Russia.

*To whom correspondence should be addressed.